

Ultrasonic, Refractometry, FT-IR and DFT Studies on Hydrogen Bonding Interactions of Ethylene Glycol/Hexanol Binary Mixtures

K. SRISANTHI¹, T. VISHWAM² and S. SREEHARI SASTRY^{1,2}

¹Department of Physics, Acharya Nagarjuna University, Nagarjuna Nagar-522510, India

²Department of Physics, GITAM (Deemed to be University)-Hyderabad Campus, Rudraram, Patancheru (M)-502329, India

*Corresponding author: E-mail: sreeharisastry@yahoo.com

Received: 22 November 2021;

Accepted: 6 February 2022;

Published online: 20 April 2022;

AJC-20769

The density (ρ), ultrasonic velocity (U), viscosity (η) and refractometry (n_D) measurements are performed on the ethylene glycol/hexanol binary liquid mixtures in the range of temperatures 298.15-323.15 K. Various parameters such as adiabatic compressibility (β), acoustic impedance (Z), intermolecular free length (L_f), internal pressure (π) and relaxation time (τ) were calculated based on the experimentally determined values. The excess parameters were calculated to interpret the hydrogen bond networks and environment associated with the liquid solution. The interaction energy between the mixture components is analyzed using the DFT-B3LYP calculations using 6-311+G(d,p), 6-311++G(d,p) basis sets. The FT-IR spectra support the hydrogen bond in the system. The optimization energy, dipole moment of the components were also represented to correlate the measured parameters. The various theories of ultrasonic velocities and mixing rules for refractive index values were also attempted to estimate the ultrasonic speed, refractive index values of the ethylene glycol/hexanol binary system.

Keywords: Ethylene glycol, Hexanol, Hydrogen bond, Ultrasonic parameters, Gibbs free energy, DFT, Mixing rules.

INTRODUCTION

Ultrasonic studies of liquid binary mixtures consists of polar and non-polar components are significant in apprehending intermolecular interactions between the constituent molecules. They realized vast relevance in diverse industrial and technological processes [1,2]. Further, such studies as a function of composition bestow keen insight into the structure and bonding of molecular aggregates [3,4]. The physical characteristics of the materials are influenced by ultrasonic wave propagation, which can provide a rich wealth of information on molecular interactions in pure liquids and liquid mixtures. The variation in molecular size and strength of the molecular interaction is attributed to the sign and extent of non-linear deviations from ideal values of velocities and isentropic compressibilities of liquid mixtures with concentration [5,6]. The nature of intermolecular interaction in pure liquids [7], binary and ternary mixtures has been thoroughly elucidated using ultrasonic velocities. The technique of analyzing molecular interactions based on the fluctuation of thermodynamic parameters and

their excess values with composition [8,9] provides insight into molecular interactions.

Ethylene glycol is a colourless viscous liquid and possesses hygroscopic properties. It is miscible in all quantities with water, ethanol and has a pleasant flavour but also has a harmful impact. Ethylene glycol is a stupendous solvent used in various applications for instance tobacco humectants, suspension medium for conducting salts in electrolytic capacitors. Also, soybean foam stabilizers are utilized in fire extinguishers and explosives, plasticizers, elastomers and aromatic and paraffinic hydrocarbon separations. At the same time, hexanol is a transparent, colourless liquid utilized as a solvent for a wide range of pharmaceutical industrial applications. Wirbla *et al.* [10] measured the ultrasonic velocities and densities of ethylene glycol (EG) and polyethylene glycol (PEG) in aqueous solutions at different temperatures. Their studies revealed the compact pseudostable structure formation and their structural interactions at low concentrations. Kondaiah *et al.* [11] measured the ultrasonic velocities and densities of aqueous ethylene glycol, propylene glycol solutions at a different molar concentration in isopropanol at

308.15 K. Their studies reported that various excess and deviation parameter values attributed to strong interactions between the molecules. Also, the geometrical fitting of tiny molecules into smaller cavities causing considerable changes in the volumetric properties. Chakraborty & Juglan [12] measured the density and ultrasonic speed of EG, DEG and TEG in the hydrated solutions of glycerol in the temperature range 293.15-308.15 K. The structure building or crumbling propensity of glycols in aqueous glycerol solutions is explored with reference to the solute-solute or solute-solvent interactions using derived parameters.

Kaur *et al.* [13] measured the sound speed, density of binary mixtures of EG, DEG and TEG with glycerol at different temperatures and frequency of 2 MHz over the whole mole fraction range. The nature of the intermolecular interactions inside the mixture is depicted by the variation in sound speed with the molality of the solute in the solvent. The experimental values' divergence from the molar mass of glycols is interpreted in terms of molecular interactions among the binary mixture's components. Kothai [14] reported the ultrasonic studies of EG, DEG, TEG in ethanol medium and suggested that strong polymer-solvent interactions exist at one of the concentrations. Tsierkezos *et al.* [15] also carried out the acoustic measurements on the binary mixtures of DMSO with EG, DEG and TrEG solutions. Their study revealed that excess molar volume shows negative behaviour with increase in glycols concentrations and results presence of heteromolecular association in the solution. Linde & Palaiologou [16] observed that the presence of a compacted pseudostable structure at extremely low concentrations in ethylene glycol and polyethylene glycols solutions while studying the ultrasonic properties. Kaur *et al.* [17] carried out the volumetric study and ultrasonic study of EGs in aqueous glycerol solutions in the temperature range of 293.15-308.15 K. Their studies revealed that the structure breaking propensity of glycols in aqueous glycerol medium influence the acoustic and isentropic compression properties.

The available literature deals with the acoustic and viscosity studies of the mixture of changing composition at a specified temperature but not on the temperature-dependent thermodynamic, viscosity, refractometry and volumetric properties. This factor has driven us to study the density, volumetric, thermodynamic, refractometry and density functional studies (DFT) of ethylene glycol/hexanol binary mixtures. The aim behind the present study is to recognize (i) molecular interaction among the components present in the solution as to hydrogen bond (ii) identify the congenital bestowal based on volumetric parameters; and (iii) the effect of hydrogen bonding on acoustic viscosity behaviour and thermodynamic values.

In present work, we report the volumetric, acoustic, viscosity, refractometry and thermodynamic properties of the ethylene glycol/hexanol liquid mixtures in the temperature range 298.15-323.15 K. The refractive index measurements coupled with density are very advantageous in furnishing its relevance in chemical industries. Copious mixing rules have been available in the literature, which include Lorentz [18] and Weiner [19], Heller [20], Dale & Gladstone [21]. Several investigations [22-26] were carried out to validate of the mixing principles. At temperatures ranging from 298.15 to 323.15 K, an attempt was made to investigate the refractive index mixing rules for the full composition range. A comparison is made between the experimental data and the calculated theoretical mixing values and between the practical and theoretical values, there has been a fair agreement.

EXPERIMENTAL

Chemicals *viz.*, ethylene glycol (EG) and hexanol of analytical reagent grade were acquired from Sigma-Aldrich, India. These chemicals were much refined using a double distillation technique and collected middle fractions of the chemical compound. To limit moisture absorption, these solutions were stored in dark bottles with molecular sieves (8 Å). The EG/hexanol binary mixtures were synthesized in eleven-volume concentration ranges. Weight measurements were recorded and the corresponding mole fraction of solute (X_1) and mole fraction of solvent (X_2) were also determined. The densities (ρ) of pure and liquid binary mixtures were determined using the specific gravity bottle method. The uncertainty in the mole fractions (X_1, X_2) and the density (ρ) measurement were estimated to be less than $\pm 0.0001, \pm 0.0001 \text{ kg m}^{-3}$. The density (ρ), speed of sound (U), viscosity (η) and refractive index (n_D) values of pure liquids at room temperature are tabulated in Table-1. These values are compared with the reported values. The difference between measured and reported values was between $\pm 1-2\%$ error limits.

Measurements: A single crystal variable path interferometer (Mittal Enterprises, India) operated at a frequency of 2 MHz, was used to detect ultrasonic velocity of pure and liquid mixtures with an accuracy of 0.02%. A specific gravity bottle standard approach was used to determine the density of the mixtures. The uncertainty in density be $\pm 0.001 \text{ kg/m}^3$. The temperature was maintained stable by flowing water from an electronically controlled thermostatic bath (M/s Mittal Enterprises, India) throughout the measurements with an accuracy of $\pm 0.01 \text{ K}$. The viscosity of all the pure and liquid mixtures were measured with a $\pm 0.001 \text{ cP}$ accuracy using an Ostwald viscometer with a 10 mL capacity. The refractive indices

TABLE-1
EXPERIMENTAL AND LITERATURE VALUES FOR DENSITY (ρ), ULTRASONIC VELOCITY (U),
REFRACTIVE INDEX (n_D), AND VISCOSITY (η) OF THE PURE LIQUIDS AT 298.15 K

Liquid sample	Source/Purity	Density (g/cm^3)		Ultrasonic velocity (m/s)		Refractive index		Viscosity (mPa s)	
		This work	Literature	This work	Literature	This work	Literature	This work	Literature
Ethylene glycol	Sigma-Aldrich/99.5%	1.109711	1.10980	1655.6	1654.35	1.4318	1.4304	16.63055	16.8388
Hexanol	Sigma-Aldrich/99.5%	0.815185	0.81523	1302.84	1304.72	1.418	1.41603	4.538447	4.594

of the above-mentioned mixtures were determined using a thermostated, very precise Abbe's refractometer over the required temperature range.

Determination of ultrasonic and volumetric parameters:

Excess molar volume (V_m^E), partial molar volume ($V_{m,i}$), apparent molar volume ($V_{\phi,i}$) and coefficient of thermal expansion (α_p) [27] were analyzed and reported in Table-2 based on volume fraction and density data at varied temperatures, *i.e.* 298.15 to 323.15 K. The observed ultrasonic velocity and density data were used to calculate the acoustic impedance (Z), adiabatic compressibility (β), intermolecular free length (L_f), internal pressure (π) and relaxation time (τ) of the EG + hexanol binary mixtures at various temperatures [28]. The chosen system's molar refraction (R_m) [29], molar polarization (P_m) [30] and excess refractive index (n_D^E) [31] were also computed to interpret the molecular interactions. The details procedure for the evaluation of this parameters was explained earlier [32].

The different mixing rules for envisaging the ultrasonic velocities and refractive index (n) of EG + hexane binary mixtures are mentioned below.

Theories of ultrasonic velocities

Nomoto's relation: On presuming the additivity of molar sound velocity (R) and the volume does not vary on mixing [33], molar sound velocity is given by:

$$R = \frac{M}{\rho U^{1/3}} \quad (1)$$

$$\text{where } M = (X_1 M_1 + X_2 M_2) \quad (2)$$

M is mean molecular weight, M_1, M_2 are the molecular weights of constituents 1 and 2.

X_1, X_2 are the Mole fractions of the components 1 & 2.

$$U_{NR} = \left(\frac{X_1 R_1 + X_2 R_2}{X_1 V_1 + X_2 V_2} \right)^3 \quad (3)$$

Impedance relation: Impedance is the product of acoustic velocity and the density of chosen mixture [34] and the relation is given by:

$$U_{IR} = \frac{\sum X_i Z_i}{\sum X_i \rho_i} \quad (4)$$

TABLE-2
DENSITY (ρ), EXCESS MOLAR VOLUME (V_m^E), PARTIAL MOLAR VOLUME ($V_{m,1}, V_{m,2}$), APPARENT MOLAR VOLUME ($V_{\phi,1}, V_{\phi,2}$) AND COEFFICIENT OF THERMAL EXPANSION (α_p) FOR THE BINARY MIXTURES OF EG AND HEXANOL AT TEMPERATURES 298.15-323.15 K

X_1	ρ (g cm ⁻³)	V_m^E (cm ³ mol ⁻¹)	$V_{m,1}$ (cm ³ mol ⁻¹)	$V_{m,2}$ (cm ³ mol ⁻¹)	$V_{\phi,1}$ (cm ³ mol ⁻¹)	$V_{\phi,2}$ (cm ³ mol ⁻¹)	$\alpha_p \times 10^4$ (K ⁻¹)
298.15 K							
0.0000	0.8149	0.0000	55.7581	125.3675	–	125.3675	9.17
0.1999	0.84473	0.0000	55.7583	125.3675	55.7582	125.3675	8.82
0.3598	0.87456	0.0000	55.7583	125.3675	55.7582	125.3675	8.50
0.4907	0.90439	0.0000	55.7582	125.3675	55.7582	125.3675	8.19
0.5998	0.93422	0.0000	55.7582	125.3675	55.7582	125.3675	7.91
0.6922	0.96405	0.0000	55.7582	125.3675	55.7582	125.3675	7.64
0.7713	0.99388	0.0000	55.7582	125.3676	55.7582	125.3675	7.39
0.8399	1.02371	0.0000	55.7581	125.3677	55.7582	125.3675	7.15
0.8999	1.05354	0.0000	55.7581	125.3678	55.7582	125.3675	6.93
0.9529	1.08337	0.0000	55.7582	125.3679	55.7582	125.3675	6.71
1.0000	1.1132	0.0000	55.7582	125.3680	55.7582	–	6.51
303.15 K							
0.0000	0.8113	0.0000	56.0451	125.9238	–	125.9238	9.21
0.1999	0.84092	0.0025	56.0477	125.9263	56.0577	125.9270	8.86
0.3598	0.87054	0.0039	56.0491	125.9276	56.0559	125.9299	8.53
0.4907	0.90016	0.0045	56.0497	125.9282	56.0543	125.9326	8.23
0.5998	0.92978	0.0045	56.0497	125.9283	56.0527	125.9352	7.94
0.6922	0.9594	0.0042	56.0494	125.9281	56.0513	125.9376	7.67
0.7713	0.98902	0.0037	56.0488	125.9276	56.0499	125.9398	7.42
0.8399	1.01864	0.0029	56.0480	125.9269	56.0486	125.9419	7.18
0.8999	1.04826	0.0020	56.0471	125.9261	56.0474	125.9439	6.96
0.9529	1.07788	0.0010	56.0462	125.9252	56.0462	125.9458	6.75
1.0000	1.1075	0.0000	56.0451	125.9243	56.0451	–	6.55
308.15 K							
0.0000	0.8076	0.0000	56.1617	126.5007	–	126.5007	9.25
0.1999	0.83736	-0.0064	56.1554	126.4943	56.1297	126.4927	8.90
0.3598	0.86712	-0.0099	56.1520	126.4908	56.1342	126.4852	8.57
0.4907	0.89688	-0.0114	56.1504	126.4892	56.1385	126.4783	8.26
0.5998	0.92664	-0.0116	56.1502	126.4891	56.1424	126.4717	7.97
0.6922	0.9564	-0.0108	56.1510	126.4899	56.1462	126.4656	7.70
0.7713	0.98616	-0.0093	56.1524	126.4915	56.1497	126.4599	7.44
0.8399	1.01592	-0.0074	56.1543	126.4935	56.1530	126.4545	7.20
0.8999	1.04568	-0.0051	56.1566	126.4959	56.1561	126.4493	6.98
0.9529	1.07544	-0.0026	56.1591	126.4984	56.1590	126.4445	6.76
1.0000	1.1052	0.0000	56.1618	126.5012	56.1618	–	6.56

313.15 K							
0.0000	0.8039	0.0000	56.3708	127.0830	–	127.0830	9.30
0.1999	0.83362	-0.0096	56.3614	127.0733	56.3227	127.0709	8.94
0.3598	0.86334	-0.0149	56.3561	127.0680	56.3295	127.0597	8.61
0.4907	0.89306	-0.0172	56.3538	127.0657	56.3359	127.0492	8.29
0.5998	0.92278	-0.0174	56.3535	127.0655	56.3419	127.0395	8.00
0.6922	0.9525	-0.0162	56.3547	127.0668	56.3475	127.0303	7.73
0.7713	0.98222	-0.0140	56.3569	127.0690	56.3527	127.0216	7.47
0.8399	1.01194	-0.0111	56.3598	127.0720	56.3577	127.0135	7.23
0.8999	1.04166	-0.0077	56.3632	127.0755	56.3623	127.0059	7.00
0.9529	1.07138	-0.0040	56.3669	127.0794	56.3667	126.9986	6.79
1.0000	1.1011	0.0000	56.3709	127.0834	56.3709	–	6.59
318.15 K							
0.0000	0.8001	0.0000	56.5094	127.6865	–	127.6865	9.34
0.1999	0.82993	-0.0181	56.4914	127.6684	56.4189	127.6639	8.98
0.3598	0.85976	-0.0280	56.4816	127.6585	56.4317	127.6428	8.64
0.4907	0.88959	-0.0323	56.4773	127.6542	56.4437	127.6232	8.33
0.5998	0.91942	-0.0327	56.4768	127.6538	56.4549	127.6048	8.03
0.6922	0.94925	-0.0305	56.4790	127.6561	56.4655	127.5876	7.76
0.7713	0.97908	-0.0263	56.4831	127.6603	56.4753	127.5714	7.50
0.8399	1.00891	-0.0209	56.4886	127.6658	56.4846	127.5562	7.25
0.8999	1.03874	-0.0145	56.4950	127.6723	56.4934	127.5419	7.02
0.9529	1.06857	-0.0075	56.5020	127.6794	56.5016	127.5283	6.81
1.0000	1.0984	0.0000	56.5095	127.6870	56.5095	–	6.60
323.15 K							
0.0000	0.7962	0.0000	56.7315	128.3120	–	128.3120	9.39
0.1999	0.82599	-0.0218	56.7098	128.2901	56.6224	128.2847	9.02
0.3598	0.85578	-0.0337	56.6980	128.2782	56.6379	128.2594	8.68
0.4907	0.88557	-0.0388	56.6928	128.2731	56.6524	128.2357	8.36
0.5998	0.91536	-0.0394	56.6922	128.2726	56.6659	128.2136	8.07
0.6922	0.94515	-0.0367	56.6949	128.2753	56.6786	128.1929	7.79
0.7713	0.97494	-0.0317	56.6998	128.2804	56.6905	128.1734	7.53
0.8399	1.00473	-0.0251	56.7064	128.2870	56.7017	128.1551	7.28
0.8999	1.03452	-0.0174	56.7141	128.2948	56.7122	128.1379	7.05
0.9529	1.06431	-0.0090	56.7226	128.3034	56.7222	128.1216	6.83
1.0000	1.0941	0.0000	56.7316	128.3124	56.7316	–	6.63

Standard uncertainties u are $u(p) = 0.0002$, $u(x_i) = 0.0002$, $u(V_{m1}, V_{m2}, V_{\phi1}, V_{\phi2}) = 0.001 \text{ cm}^3 \text{ mol}^{-1}$.

Junjie's relation [35]:

$$U_j = \frac{\left(\frac{X_1 M_1}{\rho_1} + \frac{X_2 M_2}{\rho_2} \right)}{\left(\frac{X_1 V_1}{\rho_1 U_1^2} + \frac{X_2 V_2}{\rho_2 U_2^2} \right) [X_1 M_1 + X_2 M_2]^{1/2}} \quad (5)$$

Rao's specific velocity relation [36]:

$$U_R = \sum (X_i r_i d)^3 \quad (6)$$

$$r_i = \frac{U_i^{1/3}}{\rho_i} \quad (7)$$

where X_i is the mole fraction of each component; U_i is the ultrasonic velocity of each component; ρ_i is the density of each component; d is the density of mixture, respectively.

Ideal mixing relation: Van Deal & Vangeel [37] proposed a relation for the acoustic velocity as given below:

$$\frac{1}{(X_1 M_1 + X_2 M_2)} \times \frac{1}{U_{\text{imx}}^2} = \frac{X_1}{M_1 U_1^2} + \frac{X_2}{M_2 U_2^2} \quad (8)$$

where U_{imx} is the ideal mixing ultrasonic velocities of liquid mixture; U_1, U_2 are the ultrasonic velocities of each component respectively.

Refractive index mixing rules

Gladstone-Dale (G-D) [22]:

$$n_m - 1 = (n_1 - 1)\phi_1 + (n_2 - 1)\phi_2 \quad (9)$$

Newton (Nw) [22]:

$$n_m^2 - 1 = (n_1^2 - 1)\phi_1 + (n_2^2 - 1)\phi_2 \quad (10)$$

Arago-Biot (A-B) [22]:

$$n_m = n_1\phi_1 + n_2\phi_2 \quad (11)$$

Heller (H) [22]:

$$\frac{(n_m - n_1)}{n_1} = \frac{3}{2} \left[\frac{\left(\frac{n_2}{n_1} \right)^2 - 1}{\left(\frac{n_2}{n_1} \right)^2 + 2} \right] \phi_2 \quad (12)$$

Lorentz-Lorentz (L-L) [22]:

$$\frac{n^2 - 1}{n^2 + 2} = \left(\frac{n_1^2 - 1}{n_1^2 + 2} \right) \phi_1 + \left(\frac{n_2^2 - 1}{n_2^2 + 2} \right) \phi_2 \quad (13)$$

where n_m designate the refractive index of the mixture n_1, n_2 designate the refractive index of individual components and

ϕ_1, ϕ_2 designate the volume fraction of individual components respectively. The refractiveindex (n) values calculated from different mixing rules are summarized in Table-3.

The values of the root-mean-square deviation (RMSD) of the different mixing rules are calculated using the equations below and listed in Table-4.

TABLE-3
COMPARISON OF EXPERIMENTAL REFRACTIVE INDICES FROM THOSE ESTIMATED BY THE MIXING RULES PROPOSED BY GLADSTONE-DALE (G-D), NEWTON (N-W), ARAGO-BIOT (A-B), HELLER, LORENTZ-LORENTZ (L-L) FOR BINARY MIXTURE OF EG + HEXANOL AT TEMPERATURES FROM 298.15-323.15 K

X_1	$n_{mixture}$	G-D	N-W	A-B	Heller	L-L	$n_{mixture}$	G-D	N-W	A-B	Heller	L-L
		298.15 K						313.15 K				
0	1.418	1.418	1.418	1.418	1.418	1.418	1.414	1.414	1.414	1.414	1.414	1.414
0.199887	1.420	1.420	1.420	1.419	1.420	1.419	1.415	1.415	1.416	1.415	1.415	1.415
0.359838	1.421	1.421	1.421	1.421	1.421	1.421	1.417	1.417	1.417	1.417	1.417	1.417
0.490733	1.423	1.423	1.423	1.422	1.423	1.422	1.418	1.418	1.419	1.418	1.418	1.418
0.599831	1.424	1.424	1.424	1.424	1.424	1.424	1.420	1.420	1.420	1.420	1.420	1.420
0.692158	1.426	1.426	1.426	1.426	1.426	1.425	1.421	1.421	1.422	1.421	1.421	1.421
0.771304	1.427	1.427	1.427	1.427	1.427	1.427	1.423	1.423	1.423	1.423	1.423	1.423
0.839905	1.429	1.429	1.429	1.429	1.429	1.428	1.424	1.424	1.425	1.424	1.424	1.424
0.899937	1.430	1.430	1.430	1.430	1.430	1.430	1.426	1.426	1.426	1.426	1.426	1.426
0.95291	1.432	1.432	1.432	1.432	1.432	1.431	1.427	1.427	1.428	1.427	1.427	1.427
1	1.433	1.433	1.433	1.433	1.433	1.433	1.429	1.429	1.429	1.429	1.429	1.429
303.15 K						318.15 K						
0	1.417	1.417	1.417	1.417	1.417	1.417	1.412	1.412	1.412	1.412	1.412	1.412
0.199887	1.419	1.419	1.419	1.418	1.418	1.418	1.413	1.413	1.414	1.413	1.413	1.413
0.359838	1.420	1.420	1.420	1.420	1.420	1.420	1.415	1.415	1.415	1.415	1.415	1.415
0.490733	1.422	1.422	1.422	1.421	1.421	1.421	1.416	1.416	1.417	1.416	1.416	1.416
0.599831	1.423	1.423	1.423	1.423	1.423	1.423	1.418	1.418	1.418	1.418	1.418	1.418
0.692158	1.425	1.425	1.425	1.424	1.424	1.424	1.419	1.419	1.420	1.419	1.419	1.419
0.771304	1.426	1.426	1.426	1.426	1.426	1.426	1.421	1.421	1.421	1.421	1.421	1.421
0.839905	1.428	1.428	1.428	1.427	1.427	1.427	1.422	1.422	1.423	1.422	1.422	1.422
0.899937	1.429	1.429	1.429	1.429	1.429	1.429	1.424	1.424	1.424	1.424	1.424	1.424
0.95291	1.431	1.431	1.431	1.431	1.430	1.430	1.425	1.425	1.426	1.425	1.425	1.425
1	1.432	1.432	1.432	1.432	1.432	1.432	1.427	1.427	1.427	1.427	1.427	1.427
308.15 K						323.15 K						
0	1.416	1.416	1.416	1.416	1.416	1.416	1.411	1.411	1.411	1.411	1.411	1.411
0.199887	1.417	1.417	1.417	1.417	1.417	1.417	1.412	1.412	1.413	1.412	1.412	1.412
0.359838	1.419	1.419	1.419	1.419	1.419	1.419	1.414	1.414	1.414	1.414	1.414	1.414
0.490733	1.420	1.420	1.420	1.420	1.420	1.420	1.415	1.415	1.416	1.415	1.415	1.415
0.599831	1.422	1.422	1.422	1.422	1.422	1.422	1.417	1.417	1.417	1.417	1.417	1.417
0.692158	1.423	1.423	1.423	1.423	1.423	1.423	1.418	1.418	1.419	1.418	1.418	1.418
0.771304	1.424	1.424	1.424	1.424	1.424	1.424	1.420	1.420	1.420	1.420	1.420	1.420
0.839905	1.426	1.426	1.426	1.426	1.426	1.426	1.421	1.421	1.422	1.421	1.421	1.421
0.899937	1.427	1.427	1.427	1.427	1.427	1.427	1.423	1.423	1.423	1.423	1.423	1.423
0.95291	1.429	1.429	1.429	1.429	1.429	1.429	1.424	1.424	1.425	1.424	1.424	1.424
1	1.430	1.430	1.430	1.430	1.430	1.430	1.426	1.426	1.426	1.426	1.426	1.426

TABLE-4
VALUES OF RMSD AGAINST VARIOUS MIXING RULES

Theories	Ultrasonic velocities						
	298.15 K	303.15 K	308.15 K	313.15 K	318.15 K	323.15 K	
NOM	34.9	34.7	34.3	34.0	33.6	33.3	
IMP	105	106	107	108	109	110	
RAO	65.9	64.9	63.7	63.2	62.3	61.5	
JUN	13.7	14.9	16.2	17.5	18.8	20.0	
IMX	65.7	66.3	66.8	67.2	67.6	68.1	
Mixing rules	Refractive index						
	298.15 K	303.15 K	308.15 K	313.15 K	318.15 K	323.15 K	
G-D	9.135×10^{-6}	5.705×10^{-6}	0.000170949	9.045×10^{-7}	4.338×10^{-6}	8.152×10^{-6}	
Nw	2.283×10^{-5}	1.929×10^{-5}	0.000159652	1.293×10^{-5}	9.368×10^{-6}	5.705×10^{-6}	
A-B	9.269×10^{-6}	5.705×10^{-6}	0.000171054	9.045×10^{-7}	4.379×10^{-6}	8.169×10^{-6}	
H	1.057×10^{-5}	1.192×10^{-5}	0.000180846	1.629×10^{-5}	1.879×10^{-5}	2.206×10^{-5}	
L-L	4.899×10^{-6}	8.118×10^{-6}	0.000182775	1.498×10^{-5}	1.818×10^{-5}	2.220×10^{-5}	

$$\text{RMSD} = \left(\frac{1}{p} \sum (A_{\text{exp}} - A_{\text{cal}})^2 \right)^{\frac{1}{2}} \quad (14)$$

Computational details: On ethylene glycol and hexanol monomer and dimer, minimum energy-based geometry optimization and single point energy computation were accomplished by using DFT/B3LYP method with 6-311G++G(d,p) basis set [38-40]. To investigate the molecular interactions between monomers, the natural bond orbital (NBO) analysis was done on the geometrically optimized conformer structure of monomers.

RESULTS AND DISCUSSION

The measured densities (ρ), ultrasonic velocity (U), acoustic impedance (Z), viscosity (η) and relaxation time (τ) values of ethylene glycol (EG) in hexanol for all the concentrations and at temperature T = 298.15, 303.15, 308.15, 313.15, 318.15 and 323.15 K are presented in Table-5. It is noticed that the density values of binary mixture increases with the accrement in the concentration of EG and inappreciably reduces with a

rise in temperature (Fig. 1). It is attributable to the presence of mole-cular interaction within the EG and hexanol molecules. The experimental density data is compared with literature data. It is interpreted from Table-5 that the experimental density data for EG and hexanol are in coherence with the literature data [28] for various temperatures. The observed deviation from the reported literature data might be due to the deviations, which are empathized to the procedure of calibration, solution preparation its purity, various measuring methods employed. From Table-5, it is also observed that ultrasonic velocity (U), acoustic impedance (z), viscosity (η) and relaxation time (τ) increases with the increase of EG and decrease with an upsurge in temperature. The decrease in the values indicate the decrement in molecular interactions owing to thermal agitations.

The volumetric (V_m) parameters like excess molar volume (V_m^E), partial molar volume ($V_{m,i}$), apparent molar volume ($V_{\phi,i}$) and thermal expansioncoefficient (α_p) data of EG + hexanol liquid mixtures are listed in Table-2. From Fig. 2, for all the measured temperatures and concentration ranges, excess molar volume (V_m^E) has a negative value. The decrease in the total

TABLE-5
MEASURED DENSITIES (ρ), ULTRASONIC VELOCITY (U), ACOUSTIC IMPEDANCE (z), VISCOSITY (η) AND RELAXATION TIME (τ) VALUES OF EG IN HEXANOL FOR ALL THE CONCENTRATIONS AT TEMPERATURES FROM 298.15-323.15 K

X_1	ρ	U	z	η	τ	ρ	U	z	η	τ
	(kg/m^3)	(m/s)	($\text{kg/m}^2\text{s}$)	(mPa s)	(s)	(kg/m^3)	(m/s)	($\text{kg/m}^2\text{s}$)	(mPa s)	(s)
	298.15 K					313.15 K				
0	814.9	1302.84	1061684	4.538447	4.3748×10^{-9}	803.9	1252.99	1007279	2.946926	3.1132×10^{-9}
0.199887	844.73	1318.61	1113869	5.747657	5.2177×10^{-9}	833.62	1270.03	1058722	3.593004	3.5629×10^{-9}
0.359838	874.56	1339.72	1171666	6.956868	5.9093×10^{-9}	863.34	1292.77	1116100	4.239082	3.9173×10^{-9}
0.490733	904.39	1364.81	1234321	8.166078	6.4633×10^{-9}	893.06	1319.59	1178473	4.88516	4.1885×10^{-9}
0.599831	934.22	1387.44	1296174	9.375288	6.951×10^{-9}	922.78	1343.53	1239783	5.531238	4.4276×10^{-9}
0.692158	964.05	1417.98	1367004	10.5845	7.2806×10^{-9}	952.5	1375.53	1310192	6.177316	4.5702×10^{-9}
0.771304	993.88	1459.36	1450429	11.79371	7.429×10^{-9}	982.22	1418.85	1393623	6.823394	4.6011×10^{-9}
0.839905	1023.71	1499.45	1535002	13.00292	7.5325×10^{-9}	1011.94	1459.72	1477149	7.469472	4.6189×10^{-9}
0.899937	1053.54	1554.43	1637654	14.21213	7.444×10^{-9}	1041.66	1516.91	1580104	8.11555	4.5145×10^{-9}
0.95291	1083.37	1601.34	1734844	15.42134	7.4015×10^{-9}	1071.38	1565.01	1676720	8.761628	4.4519×10^{-9}
1	1113.2	1655.6	1843014	16.63055	7.2671×10^{-9}	1101.1	1620.35	1784167	9.407706	4.3389×10^{-9}
	303.15 K					318.15 K				
0	811.3	1286.36	1043624	3.894962	3.8684×10^{-9}	800.1	1236.41	989252	2.577894	2.8102×10^{-9}
0.199887	840.92	1302.31	1095139	4.866822	4.5499×10^{-9}	829.93	1253.93	1040674	3.123375	3.1914×10^{-9}
0.359838	870.54	1324.21	1152778	5.838681	5.0998×10^{-9}	859.76	1277.15	1098042	3.668856	3.4883×10^{-9}
0.490733	900.16	1349.62	1214874	6.810541	5.5383×10^{-9}	889.59	1304.55	1160515	4.214337	3.7116×10^{-9}
0.599831	929.78	1372.71	1276318	7.782401	5.9226×10^{-9}	919.42	1328.89	1221808	4.759819	3.9087×10^{-9}
0.692158	959.4	1403.98	1346978	8.75426	6.1722×10^{-9}	949.25	1361.36	1292271	5.3053	4.0209×10^{-9}
0.771304	989.02	1446.03	1430153	9.72612	6.2707×10^{-9}	979.08	1405.29	1375891	5.850781	4.0346×10^{-9}
0.839905	1018.64	1486.38	1514086	10.69798	6.3381×10^{-9}	1008.91	1446.41	1459298	6.396262	4.0404×10^{-9}
0.899937	1048.26	1542.12	1616543	11.66984	6.2416×10^{-9}	1038.74	1504.31	1562587	6.941743	3.9375×10^{-9}
0.95291	1077.88	1589.43	1713215	12.6417	6.19×10^{-9}	1068.57	1552.76	1659233	7.487224	3.8748×10^{-9}
1	1107.5	1643.99	1820719	13.61356	6.0641×10^{-9}	1098.4	1608.51	1766787	8.032706	3.7687×10^{-9}
	308.15 K					323.15 K				
0	807.6	1269.64	1025361	3.361538	3.4429×10^{-9}	796.2	1219.87	971260	2.264387	2.5482×10^{-9}
0.199887	837.36	1285.99	1076837	4.17624	4.021×10^{-9}	825.99	1237.84	1022443	2.703041	2.8477×10^{-9}
0.359838	867.12	1308.45	1134583	4.990942	4.4826×10^{-9}	855.78	1261.61	1079661	3.141695	3.0753×10^{-9}
0.490733	896.88	1334.69	1197057	5.805644	4.845×10^{-9}	885.57	1289.54	1141978	3.580349	3.2417×10^{-9}
0.599831	926.64	1358.2	1258562	6.620346	5.1639×10^{-9}	915.36	1314.28	1203039	4.019003	3.3891×10^{-9}
0.692158	956.4	1389.74	1329147	7.435048	5.3668×10^{-9}	945.15	1347.21	1273316	4.457657	3.4648×10^{-9}
0.771304	986.16	1432.43	1412605	8.24975	5.4361×10^{-9}	974.94	1391.75	1356873	4.89631	3.4571×10^{-9}
0.839905	1015.92	1473.04	1496491	9.064452	5.4827×10^{-9}	1004.73	1433.12	1439899	5.334964	3.4471×10^{-9}
0.899937	1045.68	1529.52	1599388	9.879154	5.3845×10^{-9}	1034.52	1491.69	1543183	5.773618	3.3442×10^{-9}
0.95291	1075.44	1577.21	1696195	10.69386	5.3298×10^{-9}	1064.31	1539.24	1638229	6.212272	3.2848×10^{-9}
1	1105.2	1632.19	1803896	11.50856	5.2117×10^{-9}	1094.1	1596.63	1746873	6.650926	3.1795×10^{-9}

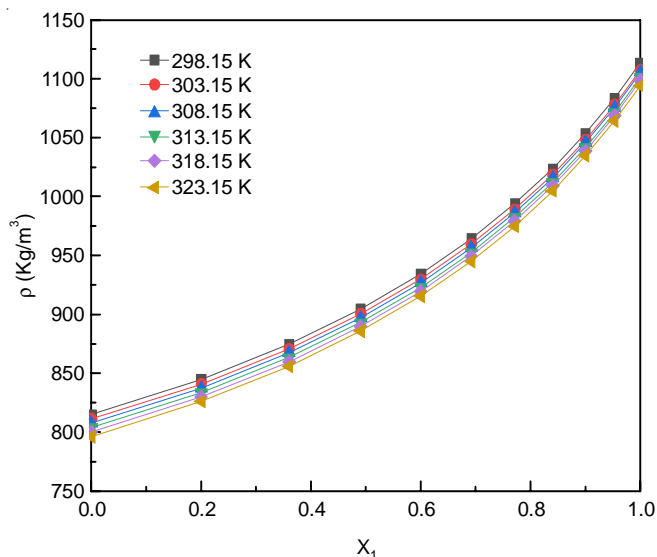


Fig. 1. Variation of density (ρ , Kg/m³) of liquid mixture with the concentration of EG at various temperatures

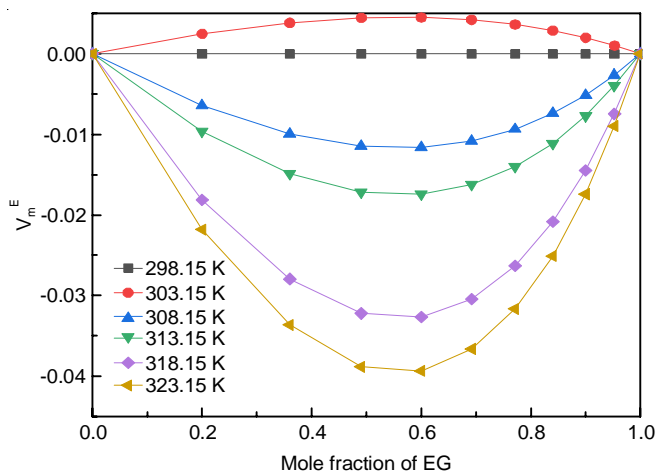


Fig. 2. Variation of excess molar volume (V_m^E) of the liquid mixture with the concentration of EG at various temperatures

molar volume of the frame is a result of simple linear summation. The stark hydrogen interaction between the EG and hexanol is responsible for the volume reduction. For all temperatures, the excess molar volume reaches a low value at equimolar concentrations of EG and hexanol, indicating compact packing of the mixture.

The establishment of a larger number of bonds or a strong intermolecular interaction between the EG and hexanol molecules *versus* the individual solute and solvent molecules occurs as the liquid combination develops. The excess molar volume decreases as the temperature is raised, which could be owing to the disruption of hydrogen bonds between the components in the mixture. As the temperature rises, the amount of hydrogen bonds in pure liquids disintegrate more easily, resulting in a greater number of free dipoles of various molecules in the binary mixture. These unbound dipoles interact with one other and form hydrogen bonds in the liquid mixture, causing a drop in effective molar volume. The partial molar volume ($V_{m,i}$) and apparent molar volume ($V_{\phi,i}$) parameters provide information

on how the solute and solvent interact in the system. It also depicts the structural organization of liquid medium, its steric hindrance property and the nature of the surrounding environment. The increase in $V_{m,1}$ and $V_{m,2}$ values is proportional to the increase in concentration of EG in the hexanol medium as well as temperature (Table-2). The rise in partial molar volume in the binary mixture suggests a difference in intermolecular interactions between the EG and hexanol molecules.

In Fig. 3, the excess thermal coefficient (α_p^E) values are negative at all concentrations and temperatures, showing a significant intermolecular interaction between EG and hexanol molecules and it behaves similarly to the excess molar volume (V_m^E) graph. A deleterious excess thermal coefficient (α_p^E) implies intermolecular interactions between various molecules, whereas a favourable α_p^E suggests self-associative interactions among the homologous molecules in the mixture, such as alcohols.

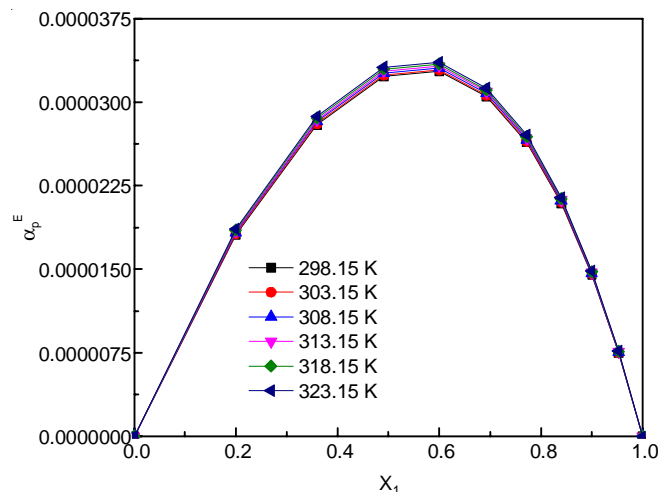


Fig. 3. Variation of excess thermal coefficient (α_p^E) of the liquid mixture with the concentration of EG at various temperatures

The formation of hydrogen bonds between distinct molecules in a liquid system is triggered by a spike in α_p^E values as temperature rises due to atoms in the liquid medium expanding their thermal vibrations. In the temperature gradient 298.15-323.15 K, the high-frequency dielectric permittivity ($\epsilon_\infty = n_D^2$) of the EG + hexanol binary system as a function of the mole fraction of EG in hexanol is shown in Fig. 4. It can be seen in graph 4 that when the amount of EG in the hexanol medium increases, the refractive index values increase.

Furthermore Fig. 4, exhibits nonlinear behaviour, indicating that heteromolecular association is occurring in the binary system. The increase in dielectric refractive index value with increasing EG concentration is due to self-associated hydrogen bond interaction between the components in the liquid mixture. When there is no heat exchange, adiabatic compressibility is the fractional decline in volume per unit rise in pressure. Also, the change in the structure is due to the change in the adiabatic compressibility. The change in the compressibility values infer a well-defined contraction on mixing and it may be due to the complex formation. From Fig. 5, it is observed that adiabatic compressibility (β) diminution with the rise in the concentra-

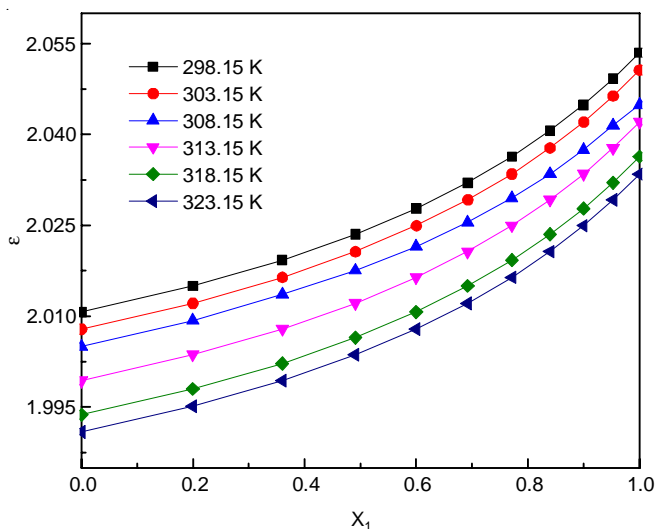


Fig. 4. Variation of high frequency dielectric permittivity (ϵ) of the liquid mixture with the concentration of EG at various temperatures

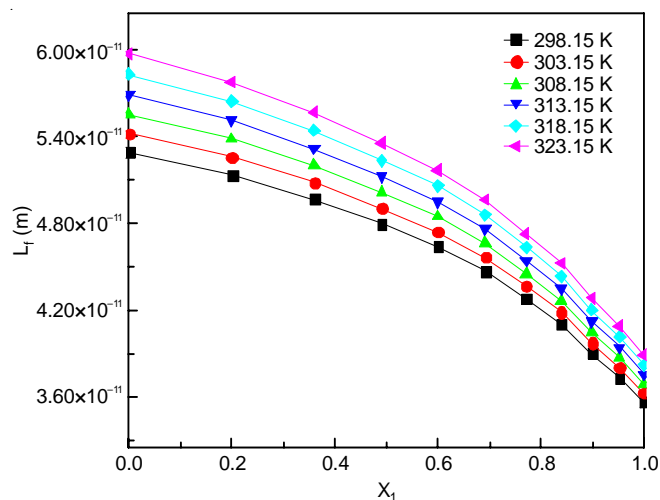


Fig. 6. Variation of intermolecular free length (L_r , m) of the liquid mixture with the concentration of EG at various temperatures

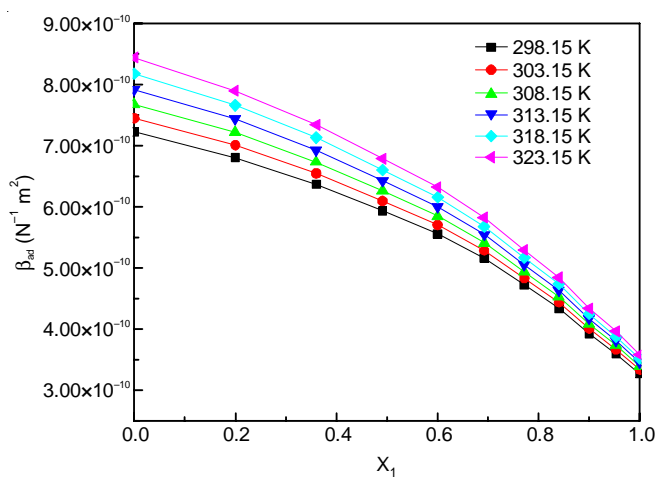


Fig. 5. Variation of adiabatic compressibility (β_{ad} , $N^{-1} m^2$) of the liquid mixture with the concentration of EG at various temperatures

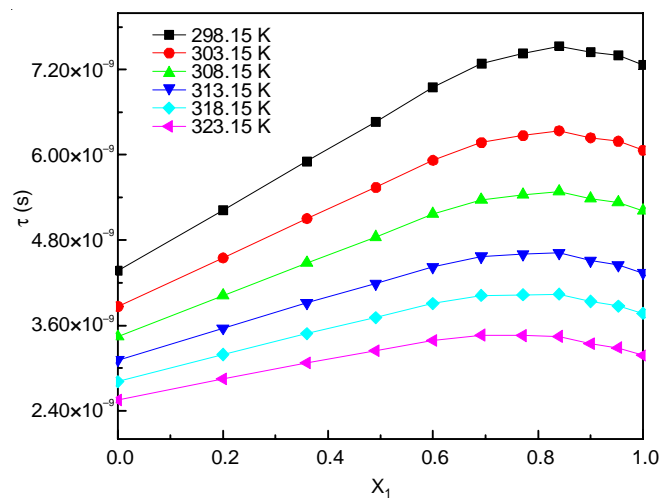


Fig. 7. Variation of relaxation time (τ , s) of the liquid mixture with the concentration of EG at various temperatures

tion of EG in hexanol medium. Moreover, there is a gradual surge in the values of compressibility with increase in temperature. This indicates the weakening of molecular interaction owing to high temperatures. The intermolecular free length (L_r) is defined as the length covered by the acoustic wave among the surfaces of the adjoining molecules. It is a degree of intermolecular interactions between the constituents of a liquid binary mixture. The increment or decrement in the values of free length suggests the weakening or strengthening of intermolecular interactions. As the acoustic velocity rises with the increase in concentration, the free length value recedes and *vice-versa*. From Fig. 6, it is marked mean free length (L_r) regresses with a rise in the concentration of EG for all the temperatures. The increment in the free length and adiabatic compressibility with increment in temperature infers the weakening of interactions at higher temperatures. Also, the relaxation time surges with the EG concentration due to the presence of hydrogen bond networks in the solution (Fig. 7).

Internal pressure is the outcome of the particle's attraction and repulsion forces. The solubility properties are also determined by internal pressure. Hydrogen bonding, charge transfer

and the Columbic (or) vander Waal interaction are all mediated by the medium's internal pressure. From Fig. 8, as the composition of EG inclines, the value of internal pressure also increases, indicating the dominance of forces of attraction. But the values of internal pressure decline with the rise of temperature. As the composition of EG inclines, the value of internal pressure also increases, indicating the closely packed nature of the molecular structure.

On the close observations of Fig. 9, it may be referred that the positive values of excess adiabatic compressibility (β^E) indicates that the intramolecular attractions in each component are weaker than the attractive forces between the molecules of the components. The β^E values reach their maximum value at 0.59 mole fraction for each temperature as the molefraction of EG grows. The excess acoustic impedance is negative for the chosen mixture. Based on the observations, it is pointed out that the excess intermolecular free length (L_r^E) is positive (Fig. 10) indicating that the acoustic wave requires a large space to cover. This could be because of the involvement of interactions between diverse components.

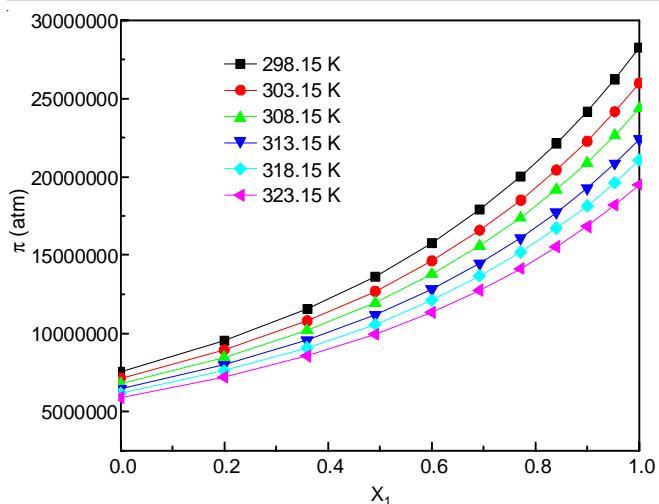


Fig. 8. Variation of internal pressure (π , atm) of the liquid mixture with the concentration of EG at various temperatures

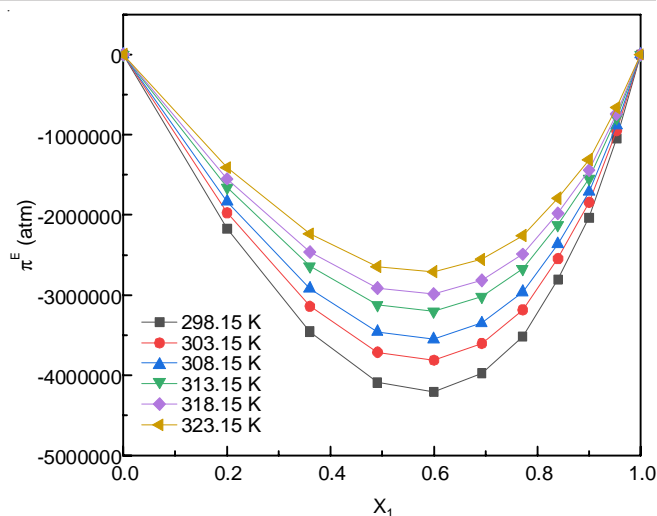


Fig. 11. Variation of excess internal pressure (π^E , atm) of the liquid mixture with the concentration of EG at various temperatures

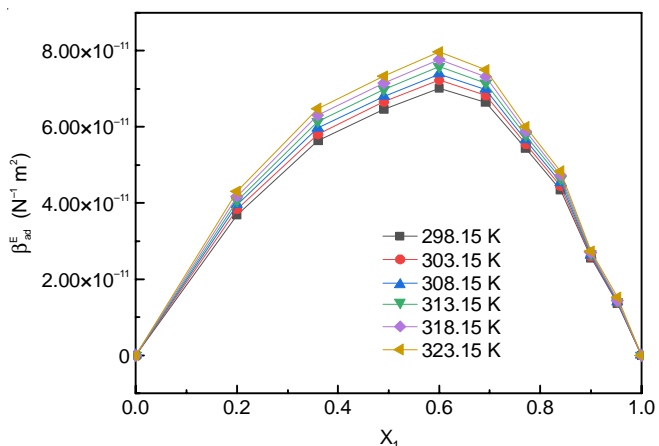


Fig. 9. Variation of excess adiabatic compressibility (β_{ad}^E , $N^{-1} m^2$) of the liquid mixture with the concentration of EG at various temperatures

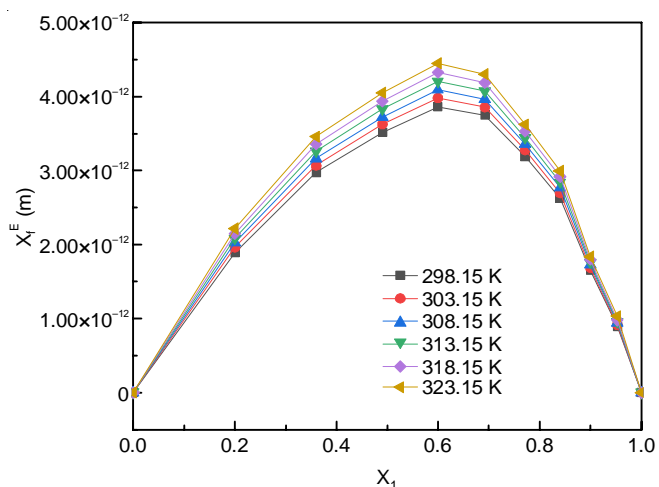


Fig. 10. Variation of excess intermolecular free length (L_r^E , m) of the liquid mixture with the concentration of EG at various temperatures

reach 0.69 mole fraction. Furthermore, the excess viscosity values are negative, indicating that the pure components have lost their dipolar interaction. It also deduces the size and shape differences among component molecules (Fig. 12).

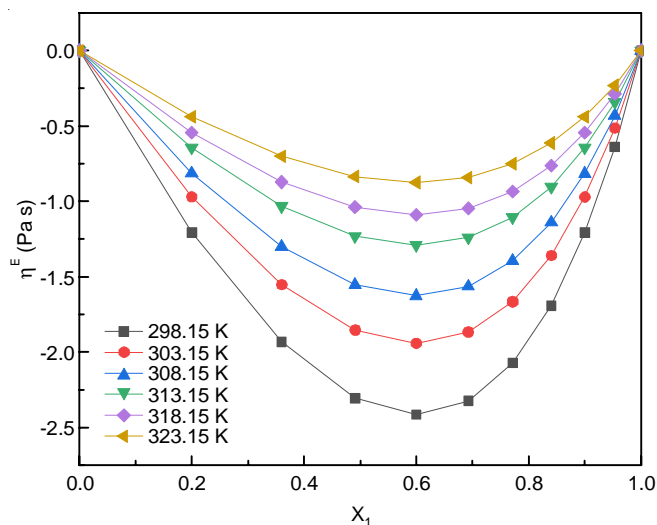


Fig. 12. Variation of excess viscosity (η^E , mPa s) of the liquid mixture with the concentration of EG at various temperatures

Fig. 11 shows the negative excess internal pressure (π^E) values indicate strong interactions between the mixture's elements. As the mole fraction of EG increases at each temperature, π^E values become progressively negative until they

Excess enthalpy is a vital thermodynamic property, which furnish information about intermolecular interactions of liquid mixtures. Excess enthalpy deliver details about complex formation, apprehend the type and strength of intermolecular interactions among unlike molecules, evaluate other thermodynamic functions, express the energy of hydrogen bonding between the constituents of the mixture. The excess enthalpy values of the present system indicates the dominance of strong intermolecular interactions. Excess Gibb's free activation energy (G^{*E}) is derived from the viscosity data. The positive excess Gibb's free energy of activation values of the present system indicate the hegemony of strong attractive forces between the unlike constituents of the mixture.

From the DFT/B3LYP single point energy calculations with different basis sets 6-311+G(d,p) and 6-311++G(d,p) (Table-6), it is observed that the energy difference between the EG + hexanol dimer and individual EG, hexanol monomers was determined to be in the order of 19-24 kcal/mol. The existence of a hydrogen connection between the EG and hexanol molecules is suggested by these energy calculations. The effect of hydrogen bonding is replicated in the frequency scale with respect to individual stretching frequencies of EG and hexanol in Fig. 13.

The FTIR spectrum of equimolar binary mixture of EG + hexanol (Fig. 14) clearly shows that there is a change in the wavenumbers of OH of EG from 3390 to 3384 cm^{-1} . It is due

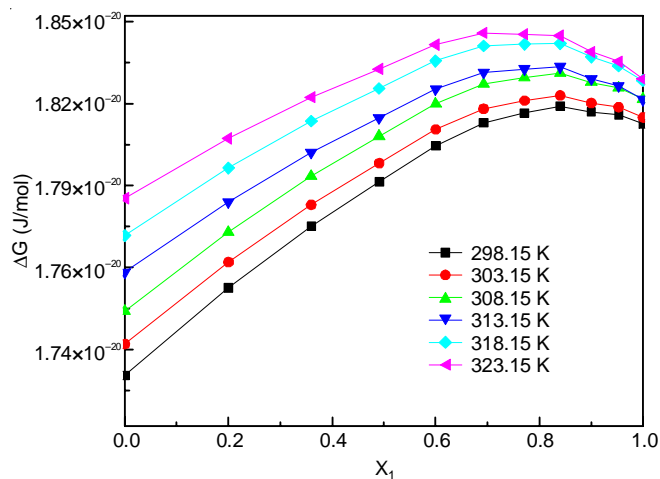


Fig. 13. Variation of Gibb's free energy (ΔG , J/mol) of the liquid mixture with the concentration of EG at various temperatures

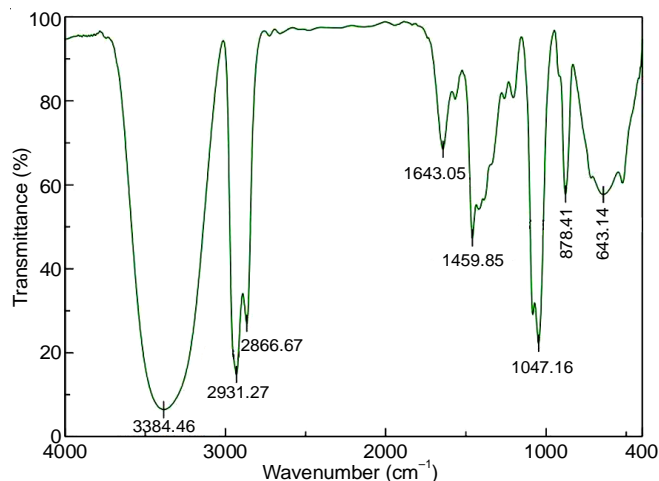


Fig. 14. FTIR spectrum of equimolar binary mixture of EG + hexanol

to the hydrogen bonding interaction between both the hydrogen atom of hydroxyl groups in EG and hexanol. This effect reduced the C-O stretching wavenumber of hexanol from 1957 to 1047 cm^{-1} . This change indicates the presence of hydrogen bonding between the EG and hexanol molecules.

The various theories were applied to estimate the ultrasonic velocities such as Nomoto (NOM), impedance relation (IMP), Rao's relation (RAO), Junjie's relation (JUN), Van Deal and Vangeel ideal mixing relation (IMX). Similarly, the different mixing rules proposed by Lorentz-Lorentz (L-L), Gladstone-Dale (G-D), Newton (N-W), Arago-Biot (A-B), Heller (H) are employed for the binary mixture of EG + hexanol to predict the refractive index values at various temperatures ranging from 298.15-323.15 K, which are tabulated in Tables 7 and 8

TABLE-6
SINGLE POINT ENERGY AND DIFFERENCE IN ENERGY OF ETHYLENE GLYCOL, HEXANOL AND THEIR EQUIMOLAR BINARY SYSTEMS AT 298.15 K

Single point energy	Gaseous state	
	DFT/B3LYP	
	6-311G + G(d,p)	6-311G + G(d,p)
Ethylene glycol (EG) energy (a.u), E_{EG}	-230.3073	-230.3256
Hexanol energy (a.u), E_{Hex}	-312.3820	-312.4463
Equimolar binary mixtures (EG + Hex) energy (a.u) E_{EG+Hex}	-542.7207	-542.7335
The difference in energy (kcal/mol); $E_T = E_{EG+Hex} - (E_{EG} + E_{Hex})$	19.73	24.13
Uncertainties in energy $u(E) = 0.0002$		

TABLE-7
COMPARISON OF EXPERIMENTAL ULTRASONIC VELOCITY FROM THOSE ESTIMATED BY VARIOUS THEORIES SUCH AS NOMOTO (NOM), IMPEDANCE RELATION (IMP), RAO'S RELATION (RAO), JUNJIE'S RELATION (JUN), VANDEAL AND VANGEEL IDEAL MIXING RELATION (IMX) FOR BINARY MIXTURE OF EG AND HEXANOL AT TEMPERATURES FROM 298.15-323.15 K

X_1	298.15 K						313.15 K					
	Exp.	NOM	IMP	RAO	JUN	IMX	Exp.	NOM	IMP	RAO	JUN	IMX
	0	1302.8	1302.84	1302.8	1302.8	1302.8	1302.84	1252.99	1253	1252.99	1252.99	1253
0.199887	1318.6	1335.714	1354.6	1318.6	1316.3	1392.36	1270.03	1286.9	1307.29	1270.03	1266.8	1346.485
0.359838	1339.7	1369.112	1401	1339.7	1333	1455.76	1292.77	1321.5	1355.95	1292.77	1283.8	1412.583
0.490733	1364.8	1403.039	1443.1	1364.8	1353.2	1503.01	1319.59	1356.6	1399.87	1319.59	1304.4	1461.786
0.599831	1387.4	1437.498	1481.4	1387.4	1377.4	1539.58	1343.53	1392.4	1439.78	1343.53	1329.1	1499.839
0.692158	1418	1472.491	1516.5	1418	1406.1	1568.73	1375.53	1428.8	1476.24	1375.53	1358.6	1530.146
0.771304	1459.4	1508.023	1548.7	1459.4	1440.1	1592.51	1418.85	1465.8	1509.72	1418.85	1393.7	1554.853
0.839905	1499.5	1544.096	1578.5	1499.5	1480.4	1612.27	1459.72	1503.5	1540.58	1459.72	1435.5	1575.381
0.899937	1554.4	1580.715	1606.1	1554.4	1528.4	1628.96	1516.91	1541.8	1569.14	1516.91	1485.6	1592.708
0.95291	1601.3	1617.882	1631.7	1601.3	1585.9	1643.24	1565.01	1580.7	1595.65	1565.01	1546.1	1607.529
1	1655.6	1655.6	1655.6	1655.6	1655.6	1655.6	1620.35	1620.4	1620.35	1620.35	1620.4	1620.35

303.15 K							318.15 K					
0	1286.4	1286.4	1286.4	1286.4	1286.4	1286.36	1236.41	1236.41	1236.41	1236.41	1236.41	1236.41
0.199887	1302.3	1319.6	1339	1302.3	1300	1377.2	1253.93	1270.668	1291.513	1253.93	1250.265	1331.207
0.359838	1324.2	1353.4	1386.2	1324.2	1316.8	1441.5	1277.15	1305.566	1340.85	1277.15	1267.372	1398.185
0.490733	1349.6	1387.7	1428.9	1349.6	1337.1	1489.4	1304.55	1341.108	1385.366	1304.55	1288.118	1448.024
0.599831	1372.7	1422.6	1467.7	1372.7	1361.5	1526.47	1328.89	1377.302	1425.795	1328.89	1313.01	1486.555
0.692158	1404	1458.1	1503.2	1404	1390.4	1556	1361.36	1414.155	1462.717	1361.36	1342.713	1517.235
0.771304	1446	1494.1	1535.9	1446	1424.8	1580.09	1405.29	1451.671	1496.6	1405.29	1378.109	1542.241
0.839905	1486.4	1530.7	1566	1486.4	1465.6	1600.11	1446.41	1489.859	1527.828	1446.41	1420.385	1563.015
0.899937	1542.1	1567.9	1593.9	1542.1	1514.3	1617.02	1504.31	1528.723	1556.719	1504.31	1471.171	1580.547
0.95291	1589.4	1605.6	1619.8	1589.4	1572.8	1631.48	1552.76	1568.272	1583.537	1552.76	1532.763	1595.54
1	1644	1644	1644	1644	1644	1643.99	1608.51	1608.51	1608.51	1608.51	1608.51	1608.51
308.15 K							323.15 K					
0	1269.6	1269.6	1269.64	1269.64	1269.64	1269.6	1219.87	1219.87	1219.87	1219.87	1219.87	1219.87
0.199887	1286	1303.2	1323.111	1285.99	1283.34	1361.8	1237.84	1254.447	1275.737	1237.84	1233.785	1315.953
0.359838	1308.5	1337.4	1371.06	1308.45	1300.26	1427	1261.61	1289.694	1325.735	1261.61	1250.971	1383.8
0.490733	1334.7	1372.1	1414.378	1334.69	1320.75	1475.6	1289.54	1325.617	1370.83	1289.54	1271.824	1434.262
0.599831	1358.2	1407.5	1453.762	1358.2	1345.3	1513.2	1314.28	1362.223	1411.77	1314.28	1296.868	1473.262
0.692158	1389.7	1443.4	1489.762	1389.74	1374.53	1543.1	1347.21	1399.521	1449.146	1347.21	1326.789	1504.308
0.771304	1432.4	1480	1522.825	1432.43	1409.25	1567.5	1391.75	1437.517	1483.437	1391.75	1362.502	1529.608
0.839905	1473	1517.1	1553.319	1473.04	1450.56	1587.8	1433.12	1476.218	1515.033	1433.12	1405.24	1550.621
0.899937	1529.5	1554.8	1581.547	1529.52	1499.96	1604.9	1491.69	1515.633	1544.256	1491.69	1456.708	1568.353
0.95291	1577.2	1593.2	1607.765	1577.21	1559.51	1619.5	1539.24	1555.767	1571.379	1539.24	1519.321	1583.515
1	1632.2	1632.2	1632.19	1632.19	1632.19	1632.2	1596.63	1596.63	1596.63	1596.63	1596.63	1596.63

TABLE-8
REDLICH-KISTER COEFFICIENT AND STANDARD DEVIATION VALUES FOR EG +
HEXANOL BINARY MIXTURES AT DIFFERENT TEMPERATURES 298.15-323.15 K

Function	Temp. (K)	A ₀	A ₁	A ₂	A ₃	A ₄	σ
V _m ^E × 10 ⁻³	298.15	1.9000	2.6000	3.3000	-10.900	0.99038	0.10485
	303.15	2.0000	2.6000	3.3000	-11.000	0.99979	0.10606
	308.15	2.0000	2.6000	2.2000	-11.500	3.1000	0.11906
	313.15	2.0000	2.6000	3.4000	-11.200	0.93200	0.10772
	318.15	2.0000	2.6000	3.4000	-11.200	8.9176	0.10892
	323.15	2.0000	2.6000	3.0000	-11.400	1.9000	0.11566
K _s ^E × 10 ⁻¹¹	298.15	-2.2758	1.2593	2.9322	-19.481	-8.5621	0.20636
	303.15	-2.7270	1.0845	2.3755	-21.249	-7.4853	0.21466
	308.15	-3.3516	0.57821	2.2362	-22.088	-7.3849	0.23782
	313.15	-4.0093	0.14320	2.9744	-22.157	-9.8101	0.24090
	318.15	-4.6991	-0.29991	2.9763	-22.987	-10.349	0.25441
	323.15	-5.4119	-0.64827	1.7080	-24.398	-7.7047	0.28101
L _r ^E × 10 ⁻¹²	298.15	14.907	7.9135	4.8967	-6.4498	-4.1384	0.092332
	303.15	15.378	8.1499	4.8213	-7.0695	-3.7796	0.096037
	308.15	15.818	8.2691	4.8856	-7.3234	-3.7283	0.10581
	313.15	16.272	8.4348	5.3851	-7.2582	-4.8157	0.10683
	318.15	16.749	8.6119	5.5516	-7.4934	-5.0775	0.11243
	323.15	17.259	8.8495	5.0819	-7.9805	-3.7452	0.12509
η ^E	298.15	-9.2955	-3.5693	-1.3407	-0.56603	-0.29913	0.000239
	303.15	-7.4709	-2.8687	-1.0775	-0.4549	-0.2404	0.000193
	308.15	-6.2628	-2.4048	-0.9033	-0.3814	-0.2015	0.0001616
	313.15	-4.9665	-1.9071	-0.7163	-0.3024	-0.1598	0.0001287
	318.15	-4.1932	-1.6101	-0.6048	-0.2553	-0.1349	0.00010875
	323.15	-3.3720	-1.2948	-0.4864	-0.2053	-0.1085	0.000087244
Z ^E × 10 ⁵	298.15	-8.7764	-5.5963	-3.8621	1.1002	1.3795	0.042808
	303.15	-8.7850	-5.6066	-3.8218	1.1761	1.2975	0.043059
	308.15	-8.7857	-5.5824	-3.6813	1.2009	1.0295	0.045914
	313.15	-8.7764	-5.5751	-3.9140	1.0651	1.5266	0.044077
	318.15	-8.7738	-5.5665	-3.9252	1.0409	1.5665	0.04461
	323.15	-8.7808	-5.5793	-3.6312	1.1093	0.85666	0.049049
τ ^E × 10 ⁻⁹	298.15	2.9092	3.3504	2.438	-1.4764	-1.9778	0.031639
	303.15	2.5793	2.8381	1.9884	-1.3868	-1.5774	0.027308
	308.15	2.3234	2.4614	1.6931	-1.2470	-1.3212	0.025501
	313.15	2.0582	2.0638	1.4824	-1.0627	-1.2940	0.021354
	318.15	1.8696	1.8134	1.2985	-0.96260	-1.1587	0.019325
	323.15	1.6684	1.5465	0.99464	-0.89819	-0.75091	0.018214

respectively. When compared to other ultrasonic theories and mixing rules for refractive index, Junjie's relation (JUN) for ultrasonic velocities and Gladstone-Dale (G-D) proposed mixing rule for refractive index have a lower standard deviation for all temperatures (Table-4).

Conclusion

The current study investigated the volumetric, acoustic and refractometry properties of ethylene glycol/hexanol binary liquid mixtures at temperatures ranging from 298.15 to 323.15 K. To interpret molecular interactions with temperature and concentration dependence, excess parameters such as molar volume (V_m^E), adiabatic compressibility (β^E), intermolecular free length (L_f^E), internal pressure (π^E) and relaxation time (τ^E) deviations are calculated from experimental data and fitted with the Redlich-Kister polynomial equation. The excess molar volume (V_m^E), excess refractive index (n_D^E) and excess thermal coefficient (α_p^E) parameters are all negative for all temperatures and concentrations, indicating the existence of hydrogen bonding in the liquid system. The interaction energy between the ethylene glycol and hexanol molecules was determined from the DFT calculations and found to be in the range of 19-24 kcal/mol. The existence of hydrogen bonding between the molecules is sustained by this computation, which is corroborated by the FT-IR spectra. Changes in the volumetric, viscosity and thermodynamic properties were caused by hydrogen bonding between ethylene glycol and hexanol molecules. Junjie's relation (JUN) for ultrasonic velocities and Gladstone-Dale (G-D) proposed mixing rule for refractive index were appropriate for all the concentrations of ethylene glycol and hexanol binary mixtures.

ACKNOWLEDGEMENTS

One of the authors (SSS) is grateful to University Grants Commission for providing BSR Faculty fellowship No. F4-5(11)/2019(BSR), dated 17-8-2020. The authors also gratefully acknowledge University Grants Commission Departmental Special Assistance at Level I program No.: F.530/1/DSA- 1/2015 (SAP-1), dated 12 May 2015.

CONFLICT OF INTEREST

The authors declare that there is no conflict of interests regarding the publication of this article.

REFERENCES

- A.S. Reddy and M. Satyanarayana, *Eur. J. Biomed. Pharm. Sci.*, **5**, 1194 (2018).
- D. Chinnarao, C.V. Padmarao, K. Raja, M. Srilatha and B.V. Rao, *Int. J. Eng. Res. Tech.*, **9**, 94 (2020).
- S. Thirumaran, J.E. Jayakumar and B.H. Dhanasundaram, *E-J. Chem.*, **7**, 465 (2010); <https://doi.org/10.1155/2010/735216>
- M.K. Praharaaj and A. Satapathy, *Indian J. Nat. Sci.*, **10**, 19721 (2020).
- A.M. Ghosh and J.N. Ramteke, *Der Chemica Sinica*, **8**, 291 (2017).
- A. Shakila, R. Raju, T. Srinivasa Krishna, R. Dey and V. Pandiyan, *Phys. Chem. Liq.*, **58**, 263 (2020); <https://doi.org/10.1080/00319104.2018.1564752>
- A. Saini, H. Joshi, K. Kukreja and R. Dey, *J. Mol. Liq.*, **223**, 165 (2016); <https://doi.org/10.1016/j.molliq.2016.08.046>
- P. Vasanthara, V. Pandiyan and A.N. Kannappan, *J. Asian Appl. Sci.*, **2**, 169 (2009); <https://doi.org/10.3923/ajaps.2009.169.176>
- A.K. Nain, *Phys. Chem. Liq.*, **45**, 371 (2007); <https://doi.org/10.1080/00319100701230405>
- W. Zý Wirbla, A. Sikorska and B.B.J. Linde, *J. Mol. Struct.*, **743**, 49 (2005); <https://doi.org/10.1016/j.molstruc.2005.02.019>
- M. Kondaiah, K. Sreekanth and Sk. Md, *J. Chem. Pharm. Res.*, **6**, 1243 (2014).
- N. Chakraborty and K.C. Juglan, *Eur. J. Mol. Clin. Med.*, **7**, 3580 (2020).
- K. Kaur, K.C. Juglan, H. Kumar and V. Sharma, *Mater. Today Proc.*, **21**, 1875 (2020); <https://doi.org/10.1016/j.matpr.2020.01.244>
- S. Kothai, *Asian J. Chem.*, **19**, 5134 (2007).
- N.G. Tsierekzos and M.M. Palaiologou, *Phys. Chem. Liq.*, **47**, 447 (2009); <https://doi.org/10.1080/00319100802104855>
- C.E.H. Schmelzer, W. Zýwirbla, E. Rosenfeld and B.B.J. Linde, *J. Mol. Struct.*, **699**, 47 (2004); <https://doi.org/10.1016/j.molstruc.2004.04.027>
- K. Kaur, I. Behal, K.C. Juglan and H. Kumar, *J. Chem. Thermodyn.*, **125**, 93 (2018); <https://doi.org/10.1016/j.jct.2018.05.016>
- H.A. Lorentz, *The Theory of Electrons and its Applications to the Phenomena of Light and Radiant Heat*, Kessinger Publishing, Whitefish, Flathead, Montana, United States, Ed.: 2, pp. 350 (1916).
- O. Weiner, *Berichte*, **62**, 256 (1910).
- W. Heller, *Phys. Rev.*, **68**, 5 (1945); <https://doi.org/10.1103/PhysRev.68.5>
- D. Dale and F. Gladstone, *Philos. Trans.*, **148**, 887 (1958).
- K. Narendra, P. Narayanam and C. Srinivasu, *Asian J. Appl. Sci.*, **4**, 535 (2011); <https://doi.org/10.3923/ajaps.2011.535.541>
- S.S. Ubarhande, A.S. Burghate, B.N. Berad and J.D. Turak, *Rasayan J. Chem.*, **4**, 585 (2011).
- S.O. Isehunwa, E.B. Olanisebe, O.O. Ajiboye and S.A. Akintola, *Afr. J. Pure Appl. Chem.*, **10**, 58 (2015); <https://doi.org/10.5897/AJPAC2015.0613>
- R. Mehra, *Proc. Indian Acad. Sci. (Chem. Sci.)*, **115**, 147 (2003); <https://doi.org/10.1007/BF02716982>
- A.Z. Tasic, B.D. Djordjevic, D.K. Grozdanic and N. Radojkovic, *J. Chem. Eng. Data*, **37**, 310 (1992); <https://doi.org/10.1021/je00007a009>
- Q.M. Omar, J.-N. Jaubert and J.A. Awan, *Int. J. Chem. Eng.*, **2018**, 8689534 (2018); <https://doi.org/10.1155/2018/8689534>
- Ashima, K.C. Juglan and H. Kumar, *Results Chem.*, **2**, 100049 (2020); <https://doi.org/10.1016/j.rechem.2020.100049>
- L. Gunganathan and S. Kumar, *Int. J. Mater. Sci.*, **12**, 89 (2017).
- S.K. Ray, J. Rath and C. Dwivedi, *Phys. Chem. Liq.*, **39**, 227 (2001); <https://doi.org/10.1080/00319100108030341>
- S.M. Tawfik and F.M. Farag, *Egypt. J. Chem.*, **61**, 310 (2018); <https://doi.org/10.21608/ejchem.2018.2347.1195>
- S.D. Deshmukh, K.L. Pattebahadur, P.B. Undre and S.S.P.W. Khirade, *Bionano Frontier*, **8**, 223 (2015).
- O. Nomoto, *J. Phys. Soc. Jpn.*, **13**, 1528 (1958); <https://doi.org/10.1143/JPSJ.13.1528>
- R.T. Lagemann and J.E. Corry, *J. Chem. Phys.*, **10**, 759 (1942); <https://doi.org/10.1063/1.1723659>
- Z. Junjie, *J. Univ. Sci. Technol. China*, **14**, 298 (1984).
- N. Santhi, M. Emayavaramban, C. Gopi, C. Manivannan and A. Raguraman, *Int. J. Adv. Chem.*, **2**, 34 (2014); <https://doi.org/10.14419/ijac.v2i2.1851>
- W. Van Dael and E. Vangeel, in *Proceedings of the International Conference on Calorimetry and Thermodynamics*, Warsaw, Poland, p. 555 (1955).
- R.G. Parr and W. Yang, *Density-Functional Theory of Atoms and Molecules*, Oxford University Press: New York (1994).
- A.D. Becke, *J. Chem. Phys.*, **98**, 5648 (1993); <https://doi.org/10.1063/1.464913>
- C.T. Lee, W.T. Yang and R.G. Parr, *Phys. Rev. B Condens. Matter*, **37**, 785 (1988); <https://doi.org/10.1103/PhysRevB.37.785>